Proceedings of the 2008 European Materials Research Society. Symposium M.
Submitted to publication in Applied Energy

Thermopower of Bismuth (Bi) Nanowire Arrays with wire diameters between 20 and 200 nm. Interplay of quantum confinement and surface effects.

T. E. Huber,[1] A. Adeyeye,[1] T. Odufa,[1] A. Nikolaeva,[2,3] L. Konopko,[2,3] R. Johnson,[4] and M.J. Graf [4]

[1] Howard University, Washington, DC 20059-0001

[2] Academy of Sciences, Chisinau, Moldova

[3] International Laboratory of High Magnetic Fields and Low Temperatures, Wroclaw, Poland.

[4] Department of Physics, Boston College, Chestnut Hill, MA 02467

We have carried out an experimental study of the transport properties and thermopower of bismuth nanowire arrays with wire diameters of 200, 60, 35, and 18 nanometers. The results are interpreted in terms of a model of three carriers, low effective mass bulklike electrons and holes and heavy mass surface carriers. Our model is consistent with observations of the Shubnikov-de Haas oscillations of the magnetoresistance of the nanowires. The bulklike carriers, because if its low effective mass, experience quantum confinement effects that become critical for wire diameters of around 60 nm. This electronic transport model is also consistent with angle-resolved photoemission spectroscopy (ARPES) studies that have shown that Bi surfaces support a large areal density of high-effective mass carriers, occupying Rashba spin-orbit surface states, coexisting with the carriers normally present in the bulk. By fitting the model to the thermopower data, we find that the surface carriers are electrons and that these surface electrons contribute substantially to the thermopower.

I. Introduction

During the past decade, impressive progress has been made in experimental studies of electronic transport in conducting nanowires. These are systems where the charge carriers are confined in two dimensions and have the third unconfined, and so provide a promising middle ground between atomic and bulk systems. As an example, we note the recent work on carbon nanotubes [1]. The "nanomaterials" approach has generated a great deal of interest in nanostructured TE (thermoelectric). TE devices are being employed in cooling applications currently; the aim of the proposed project is to contribute to extend the cooling temperatures (currently around -100 C) to lower temperatures thereby enabling higher performance applications. TE technology can potentially be used in converting waste heat into electric power in power plants, vehicles, and to scavenge thermal energy for autonomous sensors. TE device performance is limited by the materials TE figure of merit:

$$Z = \alpha^2 \sigma / \kappa \qquad (1)$$

where α, σ, and κ are the termopower, electrical conductivity and thermal conductivity, respectively. $\kappa = \kappa_{\text{electronic}} + \kappa_{\text{thermal}}$ where $\kappa_{\text{electronic}}$ and κ_{thermal} are the electronic and phonon thermal conductivities. The best bulk traditional TE materials have Z>~ 1/T where T is the absolute temperature in kelvin (K), resulting in performances of less than 10 percent of the Carnot limit. Bulk materials used in cooling are Bi, BiSb and Bi-Te compounds. Briefly, Bi is a semimetal and a fairly good TE (ZT~0.5). The semiconductor alloys BiSb and the BiTe are excellent materials (ZT~1). It has been shown experimentally that nanostructuring allows one to achieve ZT>1 in some cases of traditional TE materials [2-4]. Appropriate nanostructuring can decrease κ_{thermal} without changing σ drastically. Another effect of nanostructuring is charge-carrier quantum confinement. Such effects occur when the confining dimension, such as the diameter *d,* becomes comparable to λ_F, where λ_F is the Fermi wavelength of the charge carriers in the material. As shown by Hicks and Dresselhaus [5] and others [6], theoretical models of the effect of quantum confinement, called quantum size effects (QSE) in Bi nanowire arrays indicate that the TE figure of merit can be raised to the required high levels by nanostructuring.

Lin, Rabin, Cronin, Ying and Dresselhaus published studies of the thermopower of Bi and BiSb nanowires[7] but these studies are restricted to nanowires with $d > 40$ nm [7]. We have performed thermopower measurements of various nanowires arrays with diameters ranging between 60 nm and 18 nm. We believe that the data for the very small wire diameters is very important. In reference 7, the data was interpreted in terms of QSE of the electrons and holes that are native to bismuth, the so called bulklike states. However, angle-resolved photoemission spectroscopy (ARPES) studies of Bi surfaces have shown that Bi nanowires support surface states, with high carrier densities of around $5\times10^{12}\,cm^{-2}$ and large effective masses [8-11]. Since the surface area of a nanowire decreases as *d*, whereas the volume decreases as d^2, the surface-to-volume ratio increases as $1/d$ for decreasing wire diameter. Clearly, states that are based on the surface can potentially be more numerous than bulk states for very small diameter nanowires and dominate the thermoelectric and transport properties. Moreover, for intermediate diameters, the surface states can be considered as an impurity; as such they would impinge on the tuning of the Fermi level especially in the case of pure Bi nanowires. We have presented preliminary results in the 2007 Fall Meeting of the Materials Research Society in Boston [12].

The outline of the paper is as follows. In Section II we examine fabrication issues related to the template method. In Section III and IV we present the measurements of magnetoresistance and thermopower of pure and doped Bi nanowires and the transport model. The Appendix, section VI is a review of quantum size effects in the case of Bi nanowires.

II. Fabrication and Characterization of Nanowire Arrays.

The template method is a two step process. The first step consists of fabricating a porous alumina plate with a regular array of small-diameter, parallel channels. The second step consists of filling the channels of the template with Bi or alloys. A scanning electron microscope (SEM) image of a nanowire array is shown in Figure 1. The porous alumina is prepared by a self-assembly process (non-lithographic) of controlled anodization of aluminum in an electrolyte. The material is called porous anodic aluminium oxide (PAAO). Two batches of PAAO were used. One batch was synthesized in the laboratory of Prof. W. Wang of Tianjin University. Another batch was supplied by Synkera Co. [13]. To fill the channels, we pressure-inject the melt of the metallic material.

III. Magnetoresistance and Shubnikov-de Haas Results.

We have studied NWAs of various diameters using the method based on Shubnikov de Haas (SdH) oscillations of the magnetoresistance (MR) that measures the spectra of Landau levels caused by an applied magnetic field [14,15]. The results that we have obtained are shown in Figure 2. As we approach the semimetal-semiconductor (SMSC) transition point from the semimetal side, see Appendix, there is a trend for a decreasing carrier density with decreasing size between bulk Bi and 80-nm-diameter wires. The straight line through the data, bottom of the figure, intersects the $p = 0$ axis at the diameter value expected for the SMSC point. There is quite good agreement between this experimental value and results of theoretical calculations based on quantum confinement, which give d_{SMSC} = 63 nm for Bi wires, like these, whose crystalline orientations are such that the trigonal axis is parallel to the wire length. Other properties of the carriers in Bi nanowires also exhibit critical behavior as the diameter approaches 60 nm. For example, the anisotropy of the hole Fermi surface (FS), as measured by the ratio of the longitudinal MR (LMR) and tranverse MR (TMR) periods, decreases for decreasing wire diameter tending to zero at the SMSC critical point. The properties of nanowires of diameter d << 60 nm, on the semiconductor side of the SMSC transition, are radically different from that of nanowires on the semimetallic side. Figure 2 also presents the results of our SdH studies in the cases where a pocket of large carrier density and high effective mass was observed, the 30-nm and 60 nm nanowires. Therefore the carriers of high density that are observed have the characteristics typical of surface states. Such surface states have been observed with other experimental methods, for example, ARPES measurements [7-10], but never using SdH methods are therefore this identification is tentative. More recent work on Bi thin films can be interpreted to show that the dynamics of the surface carriers is very complex.[16] Furtherfore, studies of the dynamics of the surface carriers in nanowires using magnetoresistance methods show that this dynamics in strongly influenced by quantum interference in the periphery.[17]To contrast the surface states to the carriers that are observed in the semimetallic side of the transition, the latter shall be referred to as bulklike carriers.

IV. Thermopower Measurements

A discussion of the relevance and shortcomings of thermopower as an experimental probe is presented in Ref. 18. Figure 2 illustrates the setup. Figure 3 presents our thermopower S data as well as data from Ref. 7. During experimental runs we measure S and R as a function of temperature in the range 4 -300 K for $B = 0$ and for $B = 0.4$ T. The phenomenologic presentation of the data is as follows. It is observed that the thermopower of small diameter Bi nanowires is proportional to temperature with a negative coefficient at low temperatures, this coefficient being -1.25 T μV/K^2, for the 60-nm sample shown in Figure 3. Below, we will argue that this feature is caused by surface states. A positive peak can be noticed in the 200-nm samples and, at intermediate temperatures, in the 60-nm sample. This feature is also observed in individual Bi nanowires [18] and has been interpreted in terms as a finite size effect associated with the limitation of the mean free path of the bulklike carriers in the nanowires.

Our quantitative interpretation of our Bi nanowire thermopower data is based on a model of three bands: surface carriers and bulklike electrons and holes. Assuming diffusive thermopower, the total thermopower S of the Bi nanowires is the weighted average of the partial thermopower of the carriers involved. $S = \dfrac{N\mu_S S_S + n\mu_E S_E + p\mu_H S_H}{N\mu_S + n\mu_E + p\mu_H}$. Here, S_S is the partial thermopower of surface carriers. S_E is the partial thermopower of bulklike electrons, and S_H is the partial thermopower of bulklike holes. T is the absolute temperature in kelvin (K). Roughly, in bulk Bi, $S_E \sim -1\ T$ μV/K^2 and $S_H \sim +3\ T$ μV/K^2 at low temperatures and saturates to a constant value at higher temperatures. In nanowires, S_E and S_H depend upon the parameters of the Fermi surface that, as we have shown in Figure 2, are diameter-dependent. This method of extracting the thermopower from SdH data is discussed in Ref. 14. μ_E and μ_H are the mobilities of bulk-like electrons and holes in the nanowires, and these parameters are also dependent upon wire diameter. N is the number of surface carriers per unit volume. Note that $\Sigma = 1.8 \times 10^{12}\ cm^{-2}$ corresponds to a volumetric density N of $1.8 \times 10^{12}\ cm^{-2} \times Area / Volume(nanowire)$, which is diameter dependent. For example, for $d = 30$ nm, we find $N = 1.3 \times 10^{18}\ cm^{-3}$. In comparison, the number of electrons n and holes p per unit volume in bulk Bi are $n = p = 3.0\times10^{17}\, cm^{-3}$ at 4 K, increasing by a factor ~10 at room temperature. n and p are diameter dependent, as shown in Figure 1, and also temperature dependent. Fletcher [19] reviews the subject of experimental and theoretical thermopower of 2D electronic systems, such as Si MOSFETS. In Figure 3, in the case of 200-nm Bi NWAs, the effect of surface carriers is negligible and the peak that is observed is caused by the interplay of bulklike electrons and holes. Therefore the thermopower with a negative slope that is observed in d < 200 nm NWA is interpreted as thermopower associated with the surface states.

Now, before discussing Figure 3 in more in detail, we discuss an ancillary experiment with 60-nm nanowires. The experiment consisted of counter-doping the surface carriers, with the electron-acceptor impurity Sn and with the electron-donor Te. Figure 4 shows the concentration of bulk carriers in bulk $Bi_{1-x}Sn_x$ [20] The decrease in the numbers of electrons as the *at.% x* increases from 0 to 0.01 shows the effect of Sn. The thermopower of bulk $Bi_{1-x}Sn_x$ is more positive than that of pure Bi because there are fewer electrons. As shown in Figure 4, we observed this effect in the intermediate (100-200 K) and high temperature (200-300 K) ranges. The opposite effect of alloying is observed with BiTe alloys in the same temperature ranges (The negative peak at 20 K is interpreted as a phonon drag peak). In 60-nm nanowires, surface carriers make a contribution at low temperatures (T < 100 K). The maximum that is observed at intermediate/high temperatures (T > 100 K) is similar to that observed in 200-nm NWAs. Therefore this feature is attributed to bulklike carriers. It is reasonable to expect that bulklike carriers are thermally excited, as for bulk Bi. What is not so obvious is that the effect of impurities is restricted to the bulklike carriers, and do not extend to surface carriers. Impurities do not appear to affect the low-temperature thermopower that is caused by diffusion effects in surface carriers.

Assuming a 2D model, diffusion thermopower, and a parabolic dispersion relation, one finds [19]:

$$S_S = (k_B^2 \pi^2 T / 3e)\left[m^*(1+p) \big/ \pi\hbar^2 \Sigma \right] \qquad (2)$$

where k_B is Boltzman's constant. The energy dependence of the mobility is E^r where r = 1. Figure 3 shows, in the range (0- 40 K) a linear fit to the thermopower at low temperatures. From S_S = -1.25 T μV/K^2, neglecting the thermopower of bulk-like carriers, and using Eq. 2, we find $\Sigma = -2 \times 10^{12} cm^{-2}$ for 60-nm Bi NWAs, in fair agreement with ARPES and SdH determinations. The sign of the partial thermopower is related unambiguously to the sign of the charge of the carriers and consequently the thermopower is instrumental in establishing the type of conductivity (type-*n* or type-*p*). Clearly, we find that the surface thermopower is type-*n*. According to our interpretation, we also find that $\Sigma = -4 \times 10^{12} cm^{-2}$ and $-2 \times 10^{13} cm^{-2}$ in 35 nm and 20 nm, respectively.

The equipment at Howard U. will allows us to use magnetic fields of up to 1.3 T. In parallel with thermopower measurements with the equipment shown in Figure 2, in the future we will conduct an experimental program where we will measure the magnetoresistance and magnetothermopower of the samples at low temperatures and high magnetic fields.

V. Conclusions and acknowledgements.

We investigated the thermopower of Bi NWAs. Measurements are interpreted in terms of a model including the thermopower contributions from both surface carriers and bulklike carriers. Doping the nanowires fails to control the surface carrier thermopower. If these results are analyzed in terms of the diffusion thermopower of surface carriers, the conclusion is they are type *n,* that is like electrons. According to our measurements, the area density of surface carriers increases for decreasing wire diameters.

This material is based upon work supported by the National Science Foundation under Grant No. NSF-DMR-0506842 and NSF-DMR-0611595, by the Division of Materials of the ARO under Grant No. DAAD4006-MS-SAH and by the Civilian Research and Development Foundation for the Independent States of the Former Soviet Union (CRDF), award #MP2-3019.

VI. Appendix.

Quantum confinement effect arise because lateral confinement in a Bi nanowire raises the zero-point energy of electrons and lowers that of the holes by the confinement energy $\pi^2 h^2/m^* d^2$, where h is Planck's constant and m^* is the corresponding carrier in-plane effective mass transverse to the wire axis. Quantum confinement can decrease the band overlap to the point that, for very fine wires, the semimetal can transform into a semiconductor. In this regard the effect of quantum confinement on Bi is similar to that of alloying it with Sb. According to the detailed model of quantum confinement-induced semimetal-to-semiconductor (SMSC) transition in Bi nanowires [31], the SMSC transition is predicted to occur at $d \sim 55$ nm for wires that are oriented along the trigonal direction. The argument for improved TE properties assumes that confinement packs the carriers into one-dimensional subbands in the gap. Let us assume that a given subband, consisting of states that differ in the quasiparticle momentum parallel to the wirelength, starts at *E*. Furthermore, we assume that the electronic system is prepared so that the Fermi level, E_F, is tuned to correspond to the energy *E*. Because the density of states (DOS) is singular ($DOS \sim [E_F - E]^{-1/2}$) for this type of system, the resistance is low and the thermopower, which is the logarithmic derivative of the DOS, is enhanced.

References

Corresponding author: T.E. Huber. **thuber@howard.edu**.

1. J.P. Small, K.M. Perez and P. Kim Phys. Rev. Lett. 91, 256801 (2003)

2.. T.C. Harman, P.J. Taylor, M.P. Wash, and B.E. LaForge, Science 297, 2229 (2002).

3. R. Venkatasubramanian, E. Siibola, T. Colpitts, and B. O'Quinn, Nature 413 597 (2001).

4.. B. Poudel, Q. Hao, Y. Ma, Y. Lan, A. Minnich, B. Yu, X. Yan, D. Wang, A. Muto, D. Vashaee, X. Chen, J. Liu, M.S. Dresselhaus, G. Chen, Z. Ren. Science. 320 634 (2008).

5. L.D. Hicks and M.S. Dresselhaus, Phys. Rev. B47, 16631 (1993).

6. Y-M Lin, X. Sun, and M.S. Dresselhaus, Phys. Rev. 62, 4610 (2000).

7. Y-M Lin, O. Rabin, S.B. Cronin, J.Y. Ying and M.S. Dresselhaus, Appl. Phys. Lett. 81 2403 (2002).

8. C.R. Ast and H. Hochst , " Fermi Surface of Bi(111) Measured by Photoemission Spectroscopy," Phys. Rev. Lett. 87, 177602 (2001).

9. J.E. Gayone, S. Agergaard, S.V. Hoffmann, and Ph. Hofmann, " Strong Energy Dependence of the Electron-Phonon Coupling Strength on Bi(100)," Phys. Rev. Lett. 91, 127601 (2003), and references therein.

10. Yu. M. Koroteev, G. Bihlmayer, J.E. Gayone, E.V. Chulkov, S. Blugel, P.M. Echenique, and Ph. Hofmann, "Strong Spin-Orbit Spiltting on Bi Surfaces," Phys. Rev. Lett. 93, 46403 (2004).

11. Ph. Hofmann, Prog. Surf. Sci. 81, 191 (2006).

12. T.E. Huber, A. Adeyeye, and T. Odunfa. "Thermopower Measurements of Small (13-60 nm) Diameter Bi Nanowires," in "Thermoelectric Power Generation," edited by T.P Hogan, J. Yang, R. Funahashi, and T. Tritt. (Mat. Res. Soc., Warrendale, 2008).

13. Synkera Corporation, Longmont, CO, USA. Date 1/4/2008. http://www.synkera.com/

14. T.E. Huber, A. Nikolaeva, D. Gitsu, L. Konopko, C.A. Foss, Jr., and M.J. Graf, Appl. Phys. Lett. 84, 1326 (2004).

15. T.E. Huber, A.A. Nikolaeva, D.V. Gitsu, L.A. Konopko, and M.J. Graf, Physica E37 194 (2007).

16. K. Behnia, L. Balicas and Y. Kopelevitch, "Signatures of electron fractionalization in ultraquantum bismuth." Science 317 1729 (2007).

17. A.Nikolaeva, D. Gitsu, L. Konopko, M.J. Graf and T.E. Huber. "Quantum interference of surface states in bismuth nanowires probed by the Aharonov-Bohm oscillation of the magnetoresistance." Phys. Rev. B77, 075332 (2008).

18. A.Nikolaeva, T.E. Huber, D. Gitsu, and L. Konopko. "Diameter dependent thermopower of Bi nanowires." Phys. Rev. B77, 035422 (2008).

19. R. Fletcher. "Magnetothermoelectric effects in semiconductor systems." Semicond. Sci. Technol 14 R1 (1999).

20. K. Tanaka, "The Transverse Galvanometric Properties of Dilute BiSn, Bi-Te, and Bi-As Alloys" J. Phys. Soc. Japan 20, 1374 (1965).

Figure Captions

Figure 1. (Left). The axis on the left: Hole density p and surface carrier density N for bulk Bi and for Bi nanowires of various diameters at low temperatures determined using the Shubnikov-de Haas method. The axis on the right: Anisotropy ratio of the SdH periods for TMR and LMR. The carrier density data for the long period FS is indicated with squares and are believed to represent bulklike carriers; the anisotropy for same carriers is indicated with triangles. The carrier density data for the short period is shown as circles and represent surface carrier. For 50-nm nanowires we observe two periods, and therefore two Fermi surfaces. Dashed lines are guides for the eye.

(Right) Representation of the surface states (solid gray) and bulklike states (patterned gray). The penetration length of the surface state in the core of the nanowire is believed to be tens of nanometers in the case of trigonal wires. The bulklike states are present in the core of the nanowires, mainly. These states might be hybridized.

Figure 2. (Left). Top of a 60 nm Bi NWA based on a Synkera's PAAO. Light spots represent the top of a Bi nanowire; dark areas represent the alumina. (Right) Sketch of equipment used.

Figure 3. Thermopower of arrays of Bi nanowires. The samples' nanochannel templates are 200-nm Anopore [12], 60-nm PAAO from Wei Wang (Tianjin U., China), and 18-nm/35-nm PAAOs from Synkera[8]. Dresselhaus' group data from Ref. 6.

Figure 4. (Left) Thermopower *S* of arrays of pure and doped Bi nanowire fabricated using 60-nm Synkera templates. (Right) Electrons and holes density in bulk $Bi_{1-x}\ Sn_x$ [14].

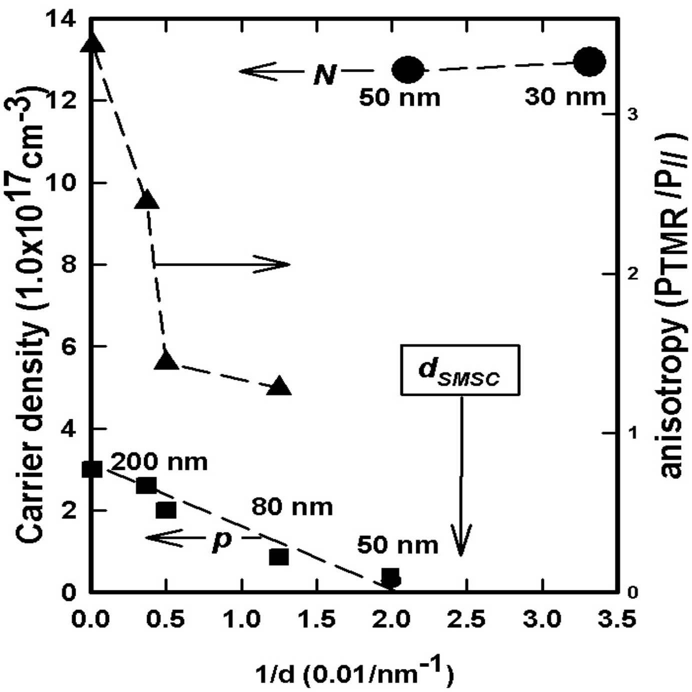

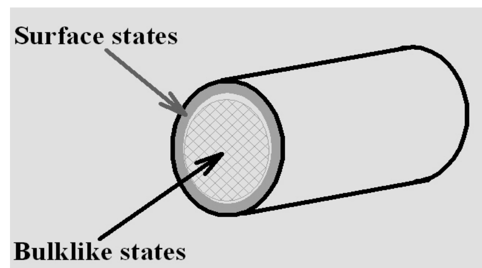

Huber. EMRS 2008.M.Figure 1

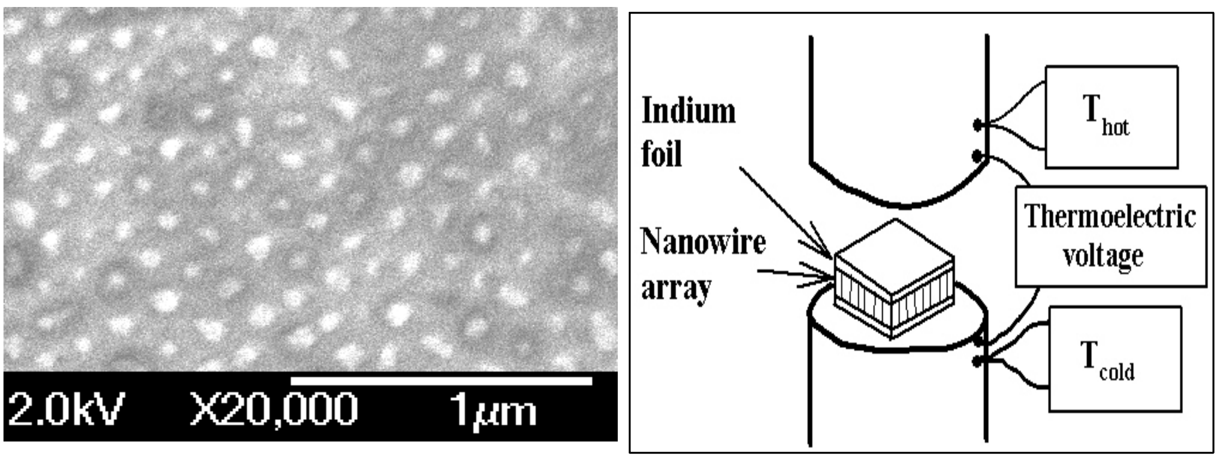

Huber. EMRS 2008.M.Figure 2

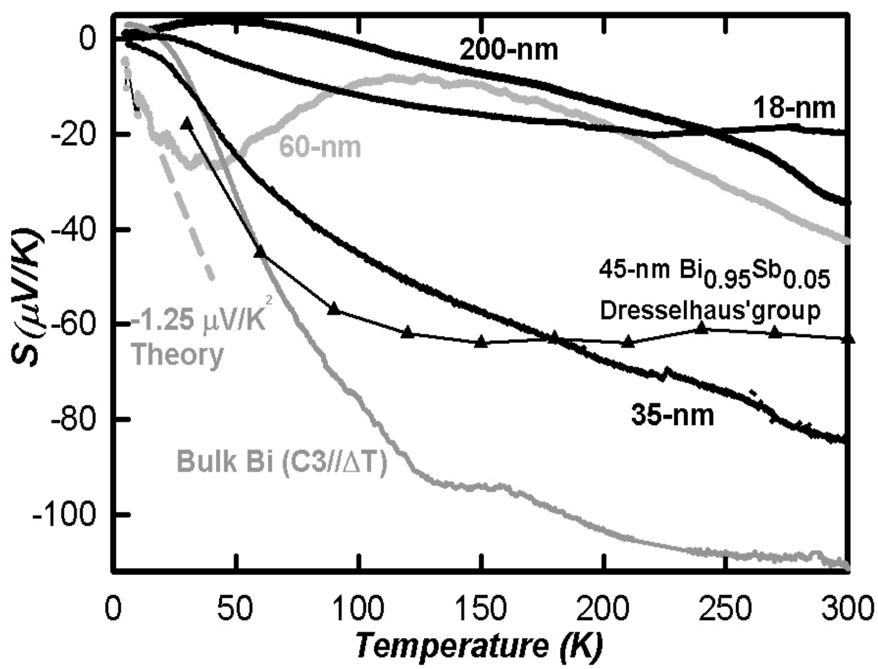

Huber. EMRS 2008.M.Figure 3

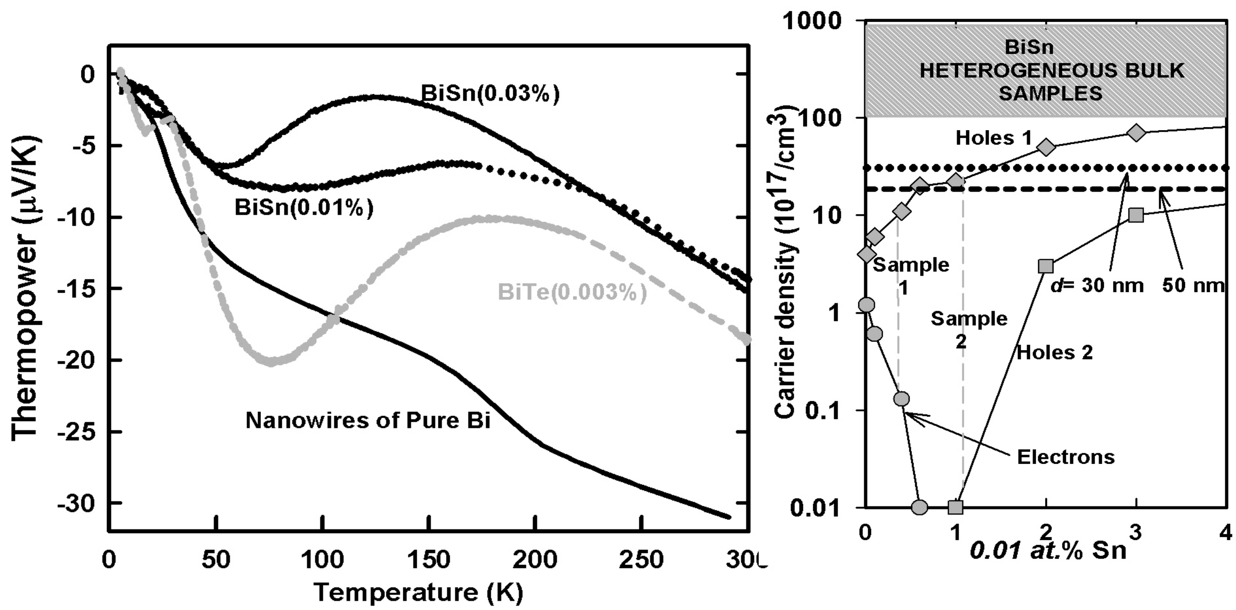

Huber. EMRS 2008.M.Figure 4